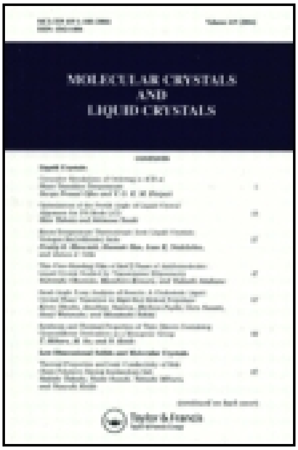

Molecular Crystals and Liquid Crystals

Publication details, including instructions for authors and subscription information:
http://www.tandfonline.com/loi/gmcl20

Molecular and Electronic Structure on n-Alkyl Cyanobiphenyl Nematogens

Steven M. Risser [a] & Kim F. Ferris [b]

[a] Core Technology Group, Battelle Memorial Institute, Columbus, OH

[b] Molecular Interactions Research Group, Pacific Northwest Laboratory, Richland, WA

To cite this article: Steven M. Risser & Kim F. Ferris (2002): Molecular and Electronic Structure on n-Alkyl Cyanobiphenyl Nematogens, Molecular Crystals and Liquid Crystals, 373:1, 143-153

To link to this article: http://dx.doi.org/10.1080/713738214

Mol. Cryst. and Liq. Cryst., 2002, Vol. 373, pp. 143-153

Molecular and Electronic Structure of n-Alkyl Cyanobiphenyl Nematogens

STEVEN M. RISSER

Battelle Memorial Institute, Core Technology Group, Columbus, OH

KIM F. FERRIS

Pacific Northwest Laboratory, Molecular Interactions Research Group, Richland, WA

First principle electronic structure calculations (*ab initio* and density functional) were performed on a series of substituted cyanobiphenyls to examine the structural and electronic properties as a function of the alkyl tail length and changes in torsion angle about the central bond connecting the rings. We find good agreement between our results and previous electronic structure studies for the optimized torsion angle between phenyls in the cyanobiphenyls, and changes in dipole moment for the cyanobiphenyls. We also find the torsion angle and rotational barriers in cyanobiphenyls to be similar to that in simple biphenyl. However, we find large discrepancies with the recent density functional calculations, which reported a much smaller torsion angle in the cyanobiphenyls.

Keywords Electronic structure, cyanobiphenyl molecules, dipole moment, liquid crystals

INTRODUCTION

There has been a recent surge of interest in the properties of liquid crystal molecules [1], due to their increased use in biologically and technologically important applications, such as electrooptical display devices [2]. The further development of these applications depends on the development of a more fundamental understanding of the relation between molecular

---

Received 23 April 2001; accepted 23 April 2001.

The authors would like to acknowledge the support of the U.S. Department of Energy, Office of Science, Materials Sciences Directorate. This work was also funded in part by the *Electroactive Coatings and Shutters for Protection of Sensors* program sponsored by DARPA through grant number DAAD-19-99-1-0003. The Pacific Northwest National Laboratory is operated by Battelle Memorial Institute for the U.S. Department of Energy under contract DE-AC06-76RLO 1830.

Address correspondence to Dr. Kim F. Ferris, Pacific Northwest National Laboratory, 902 Battelle Boulevard, P.O. Box 999, Richland, WA 99352. E-mail: kim.ferris@pnl.gov

structure and the corresponding bulk properties of the liquid crystalline mesophase, such as transition temperatures or dielectric anisotropy. This is particularly true for applications that depend on applied electric fields to induce changes in the liquid crystal phase [3–6]. In these applications, the applied electric field is coupled to the dielectric anisotropy of the phase [7] to produce a torque. The magnitude of the torque, and hence the response time of the system, is directly dependent on the dielectric anisotropy of the liquid crystal phase. The dielectric anisotropy is determined both by the electronic properties of individual molecules, such as dipole moment and anisotropy in the molecular polarizability, and by properties that are determined by the interactions between the molecules [8–10].

The ability to quantitatively predict the properties of nematic phases thus requires methods to calculate the molecular and electronic properties of single molecules, as well as the ability to describe their interaction with other molecules in the nematic phase. In this paper, we will address the first issue by examining the molecular and electronic structure of an important class of nematic molecules, the *n*-alkyl cyanobiphenyls. As is typical of many nematogens, these molecules typically consist of a central aromatic core, with one or more substituent groups appended to the core [11]. We examine the electronic and geometrical structure of these molecules using both *ab initio* and density functional methods. In the next section, we briefly describe the electronic structure methods used. We then use these methods to examine how the structural and electronic properties of the nematogens change as cyano and/or alkyl groups are appended to the aromatic core. These results are compared to previous theoretical and experimental results, and the origin of the differences between the current results and the recent work by Adam, et al. [12] are discussed. Finally, we draw some conclusions about these results, and their applicability in furthering our understanding of the molecular-level properties that determine the macroscopic behavior of liquid crystal materials.

METHODS

The initial molecular geometries for the series of cyanobiphenyls were built using default bond lengths and angles, with an initial torsion angle between the phenyls of 35°. The default geometry was then optimized using the AM1 Hamiltonian [13] as implemented in MOPAC93 [14]. The resulting structure was subsequently used as an input geometry for further electronic structure calculations.

Ab initio electronic structure calculations were performed using the Gaussian 94 [15] program. The final geometries were obtained by carrying out force optimizations [16, 48] at the Hartree-Fock level, using the 6-31G** and 6-31G* basis sets [17, 49]. Energetic barriers were obtained by performing constrained optimizations starting from the global minimum, with the single inter-ring torsion angle being used as the reaction coordinate. The potential energy surfaces were created by incrementing the torsion angle by 15°. All other coordinates were optimized at each point on the potential energy surface.

Density functional (DFT) calculations were also performed using the program DMol^3 [18] to determine the minimum energy conformation for isolated 5CB molecules. We used the DNP numerical basis (approximately comparable to the 6-31G** *ab initio* basis) [19], and the generalized gradient-corrected functional of Perdew and Wang [20]. Geometry optimizations were performed using the conjugate gradient force optimizer with default force and displacement settings.

RESULTS AND DISCUSSION

There has been extensive experimental [21–25] and theoretical research [12, 26–31] on the properties of biphenyl-based nematogens, such as the class of *n*-alkyl-cyanobiphenyls (nCB), which consist of a central biphenyl core, with a cyano (CN) group at one end, and an N-carbon alkyl chain at the other end of the core (Figure 1). The properties of the nematic phases, such as transition temperatures and dielectric anisotropy [32], strongly depend on the number of alkyl carbon atoms in the ligand. The molecular origin of these differences is still not fully understood. We have performed calculations on several molecules in the *n*CB series (0CB–6CB), as well as on 5-alkyl biphenyl (5BP), to determine whether there are observable differences in the molecular and electronic structure of the single nematogens that may explain the observed differences in the mesophases.

The structure of *n*CB is rather rigid, due to the joined pair of phenyl rings that form the biphenyl central core. The minimum energy geometry of 5CB, also shown in Figure 1, has the two phenyl rings rotated about the bond joining them, with the cyano (C≡N) group colinear with the bond linking the two phenyl rings. The alkyl tail is oriented perpendicular to the plane of the phenyl to which it is attached and is an all-*trans* conformation, although in solution this alkyl group will exhibit substantial flexibility. The magnitude of the torsion angle between the two rings strongly impacts the

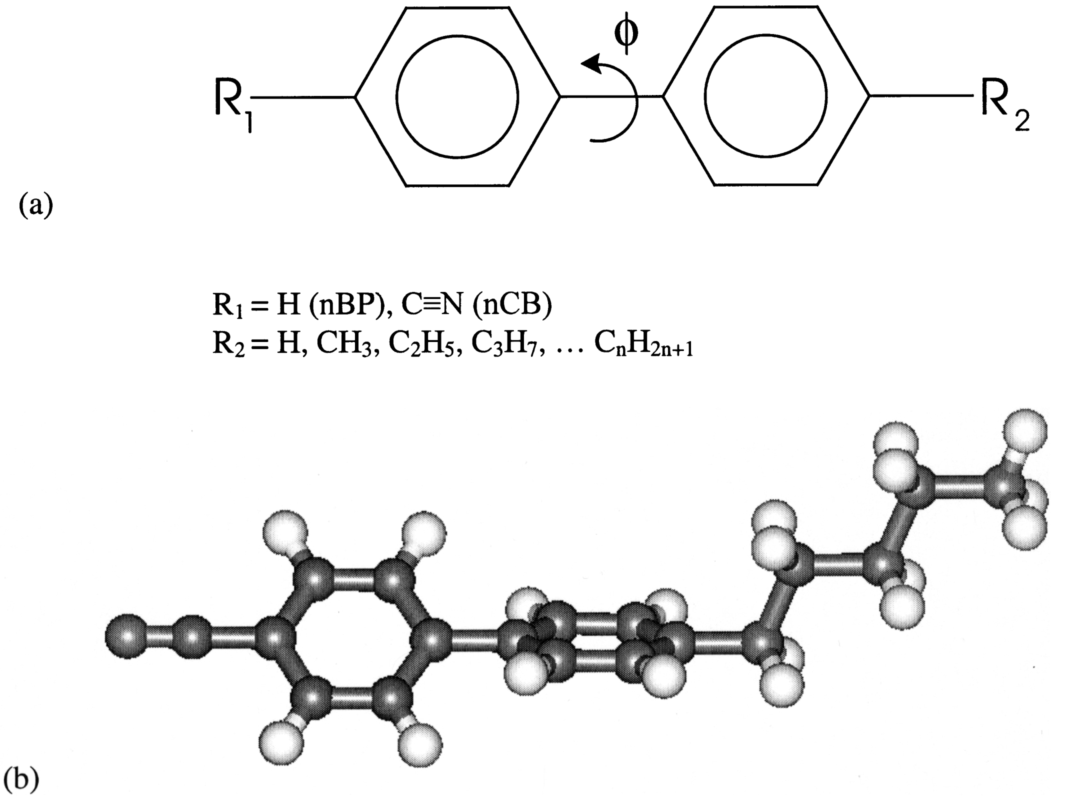

$R_1 = H$ (nBP), $C{\equiv}N$ (nCB)
$R_2 = H, CH_3, C_2H_5, C_3H_7, \ldots C_nH_{2n+1}$

FIGURE 1 (a) Schematic of the biphenyl-based nematogens, (b) Molecular structure of 5CB. $R_1 = C{\equiv}N$, $R_2 = C_5H_{11}$.

optical properties of the molecule [26, 27]. The value of this angle and the corresponding rotational barrier has been the subject of much research, particularly for biphenyl. Crystal diffraction studies have shown the rings in biphenyl (0BP) to be coplanar [33], while optical studies in solution [34, 35] suggest a torsion angle of 15–30°. Electron diffraction studies on gaseous biphenyl [36, 37] have determined a torsion angle around 45°; in good agreement with theoretical predictions of 45–46° [35, 38, 39], depending on the choice of basis set and level of correlation. The energy barriers relative to the coplanar and perpendicular cases have been determined by Raman spectroscopy [40] to be 1.00 kcal/mol and 2.03 kcal/mol, respectively. Electron diffraction measurements [36, 37] have estimated these energy differences to be 1.54 kcal/mol and 1.64 kcal/mol, and electronic structure calculations [38, 39, 41] have noted similar low barriers, depending upon both basis set extent and electron correlation. Recent high level *ab initio* calculations using correlation consistent basis sets have found these barriers to be 2.28 kcal/mol and 2.13 kcal/mol [41]. The present *ab initio* result for 5BP ($\phi_{\text{min}} = 45.49°$, Table 1) is very close to the previously reported torsion angle [39] for biphenyl of $\phi = 46.2$, using the same 6-311G** basis set.

Although the amount of previous research on the *n*CB series is less extensive, there have been previous calculations [26, 27] at lower levels of theory. Table 1 presents the torsion angle of the minimum energy structure for the *n*CB series, as well as that of 5BP, calculated using the 6-311G** basis. There is a slight decrease in the torsion angle with the addition of the first alkyl carbon; otherwise, the torsion angle is constant for the series, at approximately 44.8°. Changing to the less diffuse 6-31G* basis set, the

TABLE 1 Energy optimized phenyl-phenyl torsion angle (°) for the *n*CB series; the value for 5BP (lacking the cyano group) is also given

Molecule	*Torsion angle (°)*	*Basis set level*
0CB	44.97	6-31G*/SCF
0CB	44.24	6-31G*/MP2
0CB	46.35	6-311G*/SCF
0CB	46.09	6-311G*/MP2
0CB	45.76	6-311G**/SCF
0CB	44.76	6-311G**/MP2
1CB	44.77	6-311G**/SCF
2CB	44.80	6-311G**/SCF
3CB	44.79	6-311G**/SCF
4CB	44.76	6-311G**/SCF
5CB	44.75	6-311G**/SCF
6CB	44.75	6-311G**/SCF
5BP	45.69	6-311G**/SCF

torsion angle shows less than a full degree change. Inclusion of electron correlation at the MP2 level with accompanying geometry reoptimization resulted in very small changes in the torsion angle.

In Table 2 and Figure 2, we compare the phenyl-phenyl torsion angle for 5CB, and the energetic barriers at 0° and 90° torsion angles as determined by several electronic structure methodologies. Overall, the energetic barriers and torsion angles as determined at the 6-311G**/SCF and MP2 levels are in agreement with the precedents established by previous biphenyl investigations. It is expected that treatment of dispersive effects with more extensive basis sets and electron correlation methods would likewise reduce the energetic difference between the 0° and 90° torsion barriers.

Recently, Adam, et al. [12] reported a minimum energy torsion angle for 5CB of only 31°, calculated using density functional methods. This large discrepancy in the 5CB torsion angle between the reported DFT calculations and our current and previous results led us to question whether this difference is intrinsic to the DFT methodology. To examine the origin of this difference, we have performed DFT calculations on 5CB, using the program DMol^3 [18]. We have used the DNP numerical basis (approximately comparable to the 6-31G** *ab initio* basis) [19], and the generalized gradient corrected functional of Perdew and Wang [20]. Optimization of the geometry shows only small deviation from the *ab initio* geometry, with a minimum energy torsion angle of 43.8°. There are many possible reasons for this large discrepancy in the minimum energy torsion angle, including the use of basis, periodic boundary conditions, or choice of functionals. A more extensive investigation of these effects is currently in progress [42].

One of the most significant molecular factors determining the nature of the liquid crystalline phases is the magnitude of the permanent dipole moment and its orientation relative to the major axis of the molecule [43–45]. Nematogens that possess permanent dipole moments are more attractive for

TABLE 2 Comparison of the phenyl-phenyl torsion angle (°) and the energetic barriers at 0° and 90° for 5CB

Method	*Angle at minimum (°)*	*Barrier at* 0° *(kcal/mol)*	*Barrier at* 90° *(kcal/mol)*
ab initio/6-311G**	44.75	2.94	1.46
ab initio/6-31G*	44.07	3.09	1.71
Semiempirical/AM1	40.16	2.05	1.09
DFT/CETEP[a]	31.0		
DFT/DMol3	43.8		

[a] Value from reference [12].

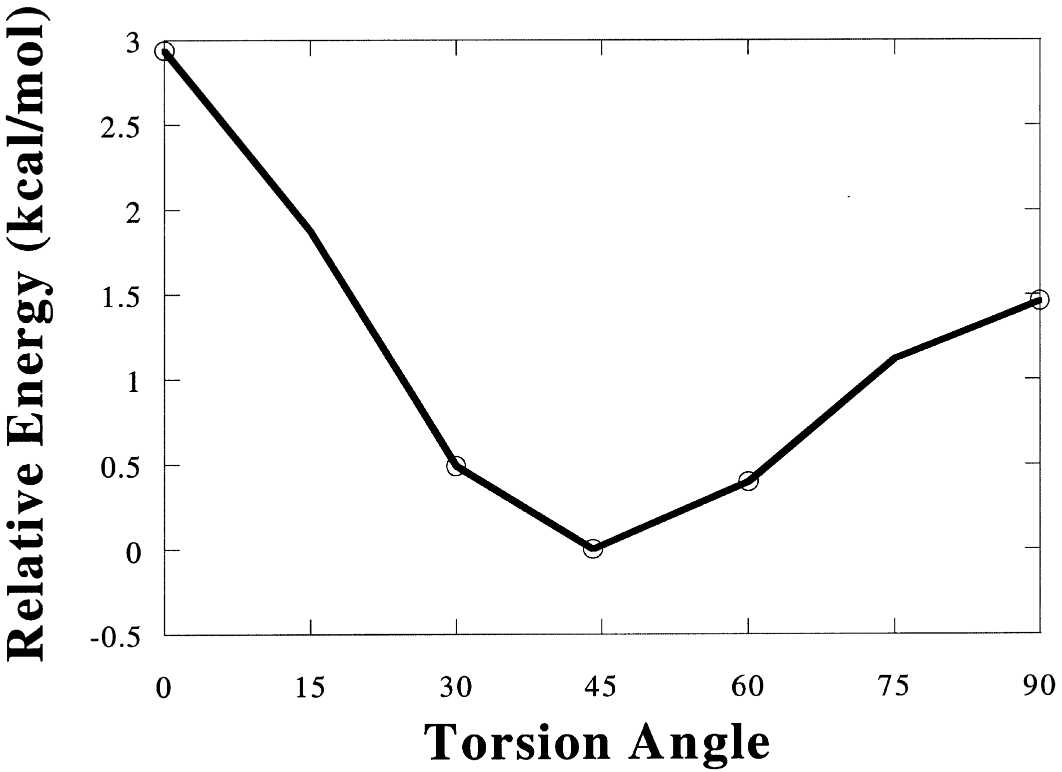

FIGURE 2 Relative total energy (kcal/mol) of 5CB as a function of the phenyl-phenyl torsion angle (°). Energies at each step are referenced to the energetic minimum at 45.76°. All coordinates other than the torsion angle were optimized at each point.

display applications and typically exhibit more phases than do nonpolar molecules [46]. Electrostatic interactions between the molecules are also significant in determining the stability of the mesophases, with dipole interactions generating up to 30% of the free energy of a phase, as has been shown in recent Monte Carlo simulations [47]. In Table 3, we show the total dipole moment for the *n*CB series, as well as 5BP. Evaluation of the dipole moment at the second order perturbation level results in an approximate 10% decrease in the dipole moment for 0CB, a result consistent with previous experience on electron correlation effects. Based on SCF results, the addition of the cyano group to biphenyl creates a large dipole of 5.43D. The addition of the electron-donating tail leads to a small increase in the dipole moment of approximately 0.53D, with the further extension of the tail producing minimal increase in the magnitude of the dipole. This is in good agreement with previous AM1 results [26], which showed similar behavior. The dipole moment of 5BP is much smaller due to the limited electron-donating ability of the alkyl carbons. It is interesting to note that the dipole moment of 5CB at the minimum energy geometry is slightly larger than the dipole moments due to the cyano group and 5-carbon alkyl tail individually, although the difference is minor. The orientation of the dipole relative to the principal molecular axes is also an important consideration, since the alignment of the nematogens in an electric field will be along the direction of the dipole. In 5CB, the dipole moment points almost exactly along the rotational axis of the phenyl rings, pointing from the cyano group to the ring terminus of the alkyl tail. The dipole moment has a small component extending along the direction of the alkyl tail.

TABLE 3 Dipole moment (Debye) at the minimum energy conformation for 5BP and the *n*CB series

Molecule	*Dipole moment (Debye)*	*Basic set level*
0CB	5.4502	6-31G*/SCF
0CB	4.9671	6-31G*/MP2
0CB	5.4400	6-311G*/SCF
0CB	4.9301	6-311G*/MP2
0CB	5.4286	6-311G**/SCF
0CB	4.8238	6-311G**/MP2
1CB	5.9586	6-311G**/SCF
2CB	5.9695	6-311G**/SCF
3CB	5.9959	6-311G**/SCF
4CB	6.0721	6-311G**/SCF
5CB	6.0576	6-311G**/SCF
6CB	6.1135	6-311G**/SCF
5BP	0.4719	6-311G**/SCF

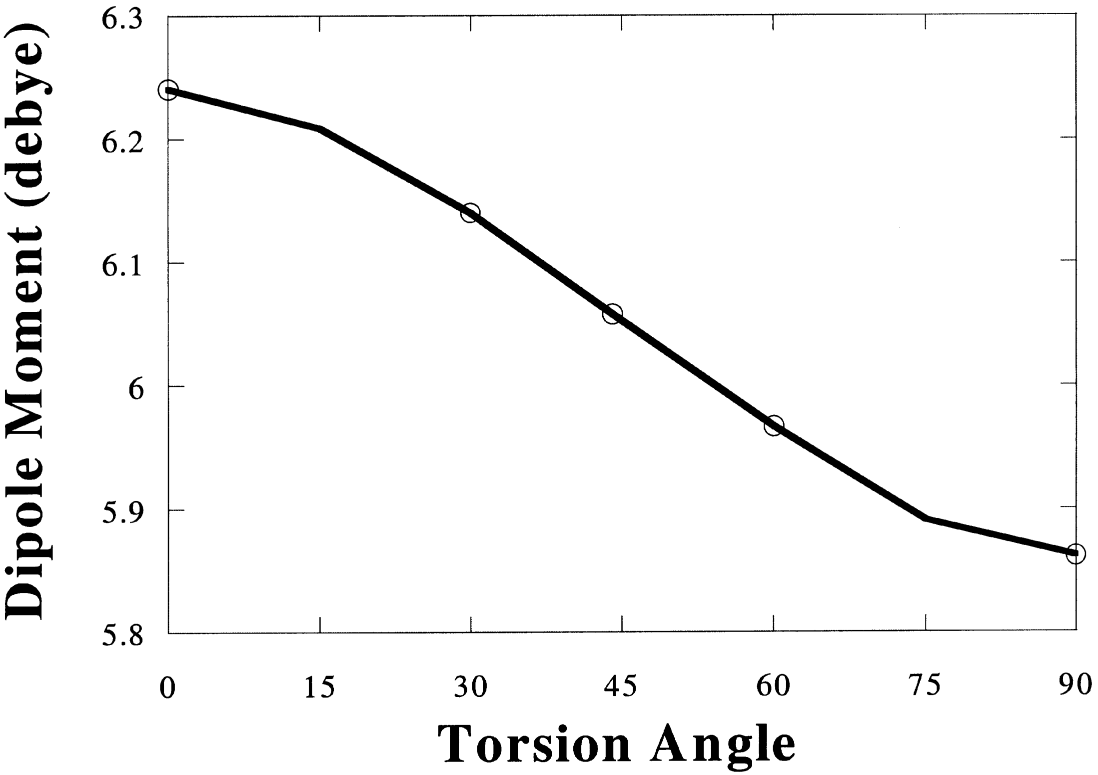

FIGURE 3 Dipole moment (Debye) of 5CB determined at the 6-311G**/SCF level as a function of the phenyl-phenyl torsion angle (°).

Although the dipole moment strongly depends on the presence of the cyano group and alkyl tail, it shows little sensitivity to the torsion angle between the rings, as shown in Figure 3. The dipole moment is largest when the rings are coplanar, having a value of 6.24D that drops to a value of 5.86D when the rings are orthogonal. The dipole moment for the 90° torsion angle is almost exactly the sum of the dipole contributions of the cyano and alkyl group contributions. This suggests that the dipole moments are simply additive when they are decoupled (rings orthogonal). More extensive conjugative interaction between the π systems of the rings (nonorthogonal phenyl-phenyl torsion angles) leads to a small enhancement of the dipole moment of the molecule. Perhaps more interesting is the nonuniform increase in the dipole moment seen in the *n*CB series, with the dipole moment of 5CB smaller than that of either 4CB or 6CB. These differences in the dipole moment between the even and odd *n*CB's have been noticed in other physical properties [8].

CONCLUSIONS

Electronic structure calculations performed on a series of alkyl-cyanobiphenyls have found that the phenyl-phenyl torsion angle is approximately 44–46°, in agreement with previous experimental and theoretical investigations on biphenyl. There is less than a 2° difference in the torsion angle between any of these molecules, with little dependence upon the length of the alkyl tall group, basis set, and electron correlation effects. These results are in close agreement with previous electronic structure calculations on 5CB, and in contrast to recent density functional results, suggesting a smaller torsion angle.

REFERENCES

1. J. W. Doane, *Mater. Res. Bull.*, 16, 22 (1991) and references therein.
2. P. J. Collings, *Liquid Crystals: Nature's Delicate Phase of Matter* (Princeton University Press, Princeton, NJ, 1990).
3. A. Gollemme, S. Zumer, and J. W. Doane, *Phys. Rev.*, A 37, 559–569 (1988).
4. I. Vilfan, M. Vilfan, and S. Zumer, *Phys. Rev.*, A 40, 4724–4730 (1989).
5. J. Bajc and S. Zumer, *Phys. Rev.*, E 55, 2925–2937 (1997).
6. H. Karacali, S. M. Risser, and K. F. Ferris, *Phys. Rev.*, E 56, 4286–4293 (1997).
7. W. Huang and G. F. Tuthill, *Phys. Rev.*, E 49, 570–574 (1994).
8. M. A. Morsy, G. A. Oweimreen, and J. S. Hwang, *J. Phys. Chem.*, 100, 8331–8334 (1996).
9. M. A. Morsy, G. A. Oweimreen, and A. M. Al-Tawfiq, *J. Phys. Chem.*, B 102, 3684–3691 (1998).

10. S. M. Kelly, *Liq. Cryst.*, 20, 493–515 (1996).
11. P. G. deGennes and J. Prost, *The Physics of Liquid Crystals*, (Oxford University Press, Oxford, UK, 1993).
12. C. J. Adam, S. J. Clark, G. J. Ackland, and J. Crain, *Phys. Rev.*, E 55, 5641–5650 (1997).
13. M. J. S. Dewar, E. G. Zoebisch, E. F. Healy, and J. J. Stewart, *J. Am. Chem. Soc.*, 107, 3902–3908 (1985).
14. J. J. P. Stewart, MOPAC 93.00 (Fujitsu Limited, Tokyo 1993).
15. M. J. Frisch, G. W. Truck, H. B. Schlegel, et al. Gaussian 94, Revision B.2, (Gaussian, Inc., Pittsburgh, PA, 1995).
16. H. B. Schlegel, *J. Chem. Phys.*, 77, 3676–3681 (1982).
17. R. Ditchfield, W. J. Hehre, and J. A. Pople, *J. Chem. Phys.* 54, 724–728 (1971); W. J. Hehre, R. Ditchfield, and J. A. Pople, *J. Chem. Phys.* 56, 2257–2261 (1972); R. Krishnan, J. S. Brinker, R. Seager, and J. A. Pople, *J. Chem. Phys.* 72, 650–654 (1980).
18. Dmol3, Cerius Version 4.2 (Molecular Simulations Incorporated, San Diego, CA, Version 4.2.1, 1999).
19. B. Delley, *J. Chem. Phys.*, 92, 508–517 (1990).
20. J. P. Perdew and Y. Wang, *Phys. Rev.*, B 45, 13244–13249 (1992).
21. G. S. Innacchione, S. Qian, D. Finotello, and F. M. Aliev, *Phys. Rev.*, E 56, 554–561 (1997).
22. K. Akasaka, M. Kimura, A. Naito, H. Kawahara, and M. Imanari, *J. Phys. Chem.*, 99, 9523–9529 (1995).
23. D. Sandstrom and M. H. Levitt, *J. Am. Chem. Soc.*, 118, 6966–6974 (1996).
24. N. Vrbancic, M. Vilfan, J. Dolinsek, G. P. Crawford, and J. W. Doane, *J. Chem. Phys.*, 98, 3540–3547 (1993).
25. D. Sandstrom, A. V. Komolkin, and A. Maliniak, *J. Chem. Phys.*, 104, 9620–9628 (1996).
26. S. M. Risser, J. Wolfgang, and K. F. Ferris, *Mol. Cryst. Liq. Cryst.*, 309, 133–142 (1998).
27. S. M. Risser and K. F. Ferris, *Nonlinear Optics*, 1, 195–200 (1991).
28. C. W. Cross and B. M. Fung, *J. Chem. Phys.*, 101, 6839–6848 (1994).
29. A. V. Komolkin, A. Laaksonen, and A. Maliniak, *J. Chem. Phys.*, 101, 4103–4116 (1994).
30. D. Sandstrom, A. V. Komolkin, and A. Maliniak, *J. Chem. Phys.*, 106, 7438–7447 (1997).
31. I. Ono and S. Kondo, *Mol. Cryst. Liq. Cryst. Lett.*, 8, 69–74 (1991).
32. A. Abe and H. Furuya, *Mol. Cryst. Liq. Cryst.*, 159, 99–114 (1988).
33. G.-P. Charbonneau and Y. Delugeard, *Acta Cryst.*, B32, 1420–1423 (1976).
34. M. Kato, M. Higashi, and Y. Taniguchi, *J. Chem. Phys.*, 89, 5417–5421 (1988).
35. Y. Takei, T. Yamaguchi, Y. Osamura, K. Fuke, and K. Kaya, *J. Phys. Chem.*, 92, 577–581 (1988).
36. A. Almenningen, O. Bastiansen, L. Fernholt, B. N. Cyvin, S. J. Cyvin, and S. Samdal, *J. Mol. Struct.*, 128, 59–76 (1985).
37. O. Bastiansen and S. Samdal, *J. Mol. Struct.*, 128, 115–125 (1985).
38. G. Hafelinger and C. Regelmann, *J. Comp. Chem.*, 8, 1057–1065 (1987).
39. J. Cioslowski and S. T. Mixon, *J. Am. Chem. Soc.*, 114, 4382–4387 (1992).
40. L. A. Carriera and T. G. Towns, *J. Mol. Struct.*, 41, 1 (1977).
41. S. Tsuzuki, T. Uchimaru, K. Matsumura, M. Mikami and K. Tanabe, *J. Chem. Phys.*, 110, 2858–2861 (1999).
42. S. M. Risser and K. F. Ferris, manuscript in preparation.
43. D. Wei and G. N. Patey, *Phys. Rev. Lett.*, 68, 2043–2045 (1992).
44. M. A. Osipov, T. J. Sluckin, and S. J. Cox, *Phys. Rev.*, E 55, 464–476 (1997).
45. L. M. Blinov, *Electrooptic Effects in Liquid Crystals* (Springer-Verlag, Berlin, 1994).
46. F. Hardouin, A. M. Levelut, M. F. Archard, and J. Sigaud, *J. Chim. Phys.*, 80, 53–64 (1981).
47. D. Levenesque, J. J. Weissm and G. J. Zarragoicoechea, *Phys. Rev.*, E 47, 496–505 (1993).
48. D. F. Shanno, *J. Optimization Theory and Applications*, 46, 87 (1985).
49. P. C. Hariharan and J. A. Pople, *Theoret. Chem. Acta* 28, 213–222 (1973).